ELSEVIER

Journal of Nuclear Materials 253 (1998) 67–77

journal of nuclear materials

Neutron irradiation effects on the density, tensile properties and microstructural changes in Hi-Nicalon™ and Sylramic™ SiC fibers

M.C. Osborne [a], C.R. Hubbard [b], L.L. Snead [b,*], D. Steiner [a]

[a] *Rensselaer Polytechnic Institute, Troy, NY 12180, USA*
[b] *Oak Ridge National Laboratory, Oak Ridge, TN, USA*

Abstract

Tensile results are presented for ceramic grade (cg) Nicalon™, Hi-Nicalon™ and Sylramic™ SiC fibers which have all been neutron irradiated in the high flux isotope reactor (HFIR) at damage levels of 0.1, 0.5, 2 and 5 dpa. Single fibers were tensile tested and the results were analyzed using Weibull statistics. Fiber axial displacements were measured with a laser micrometer which allowed for the determination of the tensile moduli. Density changes were measured with a gradient column. Transmission electron microscopy (TEM) was performed to assess microstructural damage and X-ray diffraction (XRD) was used to measure uniform strain, degree of crystallinity, average coherence length and root-mean-square microstrain. The physical and tensile results indicate that cg Nicalon™ and Hi-Nicalon™ are unstable in a neutron field. Both fiber types densify by 3–5% which would be detrimental to a composite's matrix cracking stress due to weakening or debonding of the interface. The Sylramic™ swells which is similar behavior to the monolithic SiC. The failure strength of the Sylramic™ drops by 50% after an irradiation temperature of 500°C which would have little effect on the matrix cracking condition of a composite. The Sylramic™ fiber strength decrease would significantly reduce the ultimate composite strength but the composite strength would remain above the matrix cracking strength such that the fibers may still potentially be viable for fusion applications. © 1998 Elsevier Science B.V.

1. Introduction

Silicon carbide has been discussed for fusion applications as a structural material or first wall armor for a tokamak type reactor for over 20 years [1–10]. SiC has high-temperature capabilities and low-activation properties as well as being a low Z type material (it won't impact the plasma as seriously as higher Z materials). One of the limiting factors in its use is its low fracture toughness which is 3 to 5 MPa $m^{1/2}$ depending on grain size [11,12]. For SiC/SiC continuous fiber reinforced ceramic composites (CFCCs) to be used as a structural material for fusion, an in-depth investigation into fiber and composite behavior after neutron damage is critical because various aspects of composite behavior are dependent on the fiber strength distribution.

It has been shown previously that the strength of SiC/ceramic grade (cg) Nicalon™ [1] composites is drastically changed following irradiation [13], and the initial results of low fluence neutron irradiation (< 0.5 dpa) on Hi-Nicalon™ fibers exhibited no substantial degradation of the tensile properties [14]. Therefore, this continuing research at higher doses was performed. Other SiC fibers, Sylramic™ [2] and Nicalon Type S™, have been developed which are more crystalline and have larger grains when compared to previous types such as cg Nicalon, Hi-Nicalon and Tyranno™ [3].

Continuous fiber reinforced ceramic matrix composites will have multiple matrix cracks and fiber pullout (both very dependent on interfacial properties) which contribute to more energy consumed per unit volume of specimen

* Corresponding author. Fax: +1-423 576 8424; e-mail: z2n@ornl.gov.

[1] Trademark of Nippon Carbon Co.
[2] Trademark of Dow Corning Corp.
[3] Trademark of UBE Industries.

PII S0022-3115(97)00306-1

than for the case of monolithic SiC. Using ceramic composites for fusion applications, hermeticity is important in regard to maintaining the fusion reaction in a sealed chamber; therefore changes in the matrix cracking condition must be examined. The matrix cracking condition, besides being highly dependent on interfacial properties, is also affected by fiber properties; fiber radius (r) and elastic modulus (E_f) [15]. V_f, the volume fraction of fibers, is a composite property. The relationship among the above properties has been modeled and one such model is shown in the Eq. (1) below:

$$\sigma_m = \left(\frac{6\tau G_m V_f^2 E_f E_{cl}^2}{(1 - V_f) E_m^2 r} \right)^{1/3} - \sigma_r, \quad (1)$$

where σ_m is the matrix cracking stress, σ_r is the residual stress, τ is the interfacial shear strength, G_m is the critical mode I energy release rate and E is the elastic modulus of the matrix (m) or composite. Although changes in the residual stresses will have a significant effect on any change in the matrix cracking stress, the other factors of Eq. (1) are also worth examining. Reductions in fiber moduli coupled with fiber diameter increases will reduce matrix cracking stress while increases in fiber moduli coupled with fiber shrinkage will increase the matrix cracking stress. But when examining these parameters, any change in the cracking stress will also be influenced by neutron irradiation of the interface and the matrix as well.

After multiple matrix cracking, the composite will have an ultimate failure stress (a first order estimate) which is given below:

$$\sigma_{cl}^{ult} = \sigma_b V_f, \quad (2)$$

$$\frac{\sigma_b}{\sigma_m} = \frac{(me)^{-1/m}}{\Gamma(1 + 1/m)}, \quad (3)$$

where σ_{cl}^{ult} is the ultimate strength of the composite, σ_b is the fiber bundle strength and σ_m is the fiber mean strength. A reduction in mean fiber strength reduces the ultimate composite strength. There are other more advanced theories for composite ultimate strength [16] but they will not be discussed here since Eqs. (2) and (3) will give an adequate estimate of ultimate strength changes due to neutron irradiation.

Density changes, which are related to volumetric changes, have been shown to saturate at low fluences for SiC [17–20]. Volume changes between fibers and matrix can lead to changes in interfacial properties which will affect the matrix cracking stress and fiber pullout length. Although this mismatch in expansions does not appear explicitly in the work of fracture (WOF) or pullout length (h) [21],

$$\mathrm{WOF} = \frac{V_f \sigma_f^2 r}{12\tau}, \quad (4)$$

$$h = \frac{\sigma_m^2 r}{2\tau}, \quad (5)$$

the volumetric mismatch will manifest itself in the interfacial shear strength, τ. In Eqs. (4) and (5), V_f is the volume fraction of fibers, σ_f is the fiber failure strength and h is the average pullout length.

Assuming no direct effect of neutron irradiation on the interface, swelling of the same degree between the fibers and the matrix (interface in compression) will have little effect on interfacial properties. However, fiber shrinkage coupled with matrix swelling (interface in tension) would greatly reduce interfacial strength which would lead to greater fiber pullout and lower matrix cracking stress. A major concern over changes in the critical matrix cracking stress is that the matrix cracking stress may be reduced to below the design stress in an actual component (i.e. first wall) which will result in a loss of integrity of the component. Another concern is that the ultimate composite strength and amount of pullout are greatly reduced such that the composite will completely fail without much more strain above the strain at the critical matrix cracking stress.

2. Experimental

The materials used in this study were cg Nicalon fiber, Hi-Nicalon fiber and Sylramic fiber. The compositions of these fibers are presented in Table 1 with stoichiometric SiC listed for comparison [22,23]. From Table 1, it is apparent that there is oxygen impurity in cg Nicalon fiber and excess carbon in Hi-Nicalon fiber. The oxygen in the cg Nicalon fiber arises from crosslinking of the polymer with oxygen to prevent the green fiber from melting during pyrolysis. The Hi-Nicalon fiber is crosslinked by electron radiation but if the excess carbon were driven from the fiber there would be adverse shrinkage and porosity. The Sylramic fiber has titanium and boron impurities (added to aid processing) which have formed the compound titanium diboride (TiB_2) during pyrolysis.

The cg Nicalon fiber, Hi-Nicalon fiber and Sylramic fiber tows were cut to 5 cm lengths, placed in an aluminum (graphite for the higher temperature) insert which kept the bundles separate and loaded into aluminum 'rabbit' capsules. The fibers were irradiated in the high flux isotope reactor (HFIR) in Oak Ridge, TN. They were irradiated to fluences of 1×10^{24}, 5×10^{24}, 2×10^{25} and

Table 1
Fiber compositions

Element (wt%)	cg Nicalon	Hi-Nicalon	Nicalon Type S	Sylramic	SiC
Si	56.6	63.7	68.9	66.6	70.0
C	31.7	35.8	30.9	28.5	30.0
O	11.7	0.5	0.2	0.8	
Ti				2.1	
B				2.3	
N				0.4	

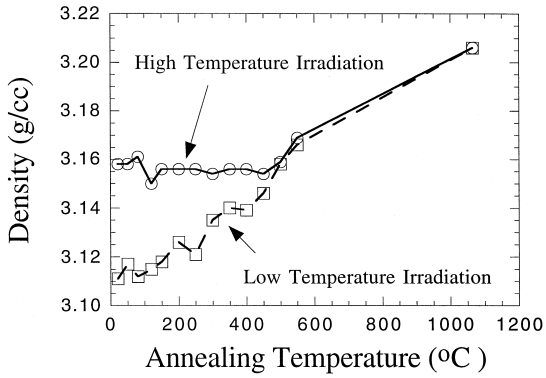

Fig. 1. Temperature monitor density versus annealing temperature.

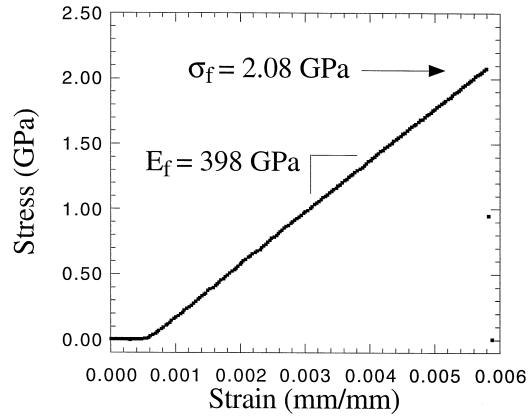

Fig. 2. Typical stress–stain curve for Sylramic fibers.

5×10^{25} n/m^2 ($E > 0.1$ MeV) and irradiation temperatures were 100–150°C and 500–550°C. The conversion from fluence to displacements per atom (dpa) used in this study was 1 dpa = 10^{25} n/m^2. Shown in Fig. 1 is a plot of the SiC temperature monitor density versus anneal temperature. From this data the appropriate irradiation temperatures are obtained [18,24]. The annealing furnace malfunctioned after the 550°C anneal, so the next annealing temperature was at 1065°C. The malfunction prevented the use of multiple points between the 550 and 1065°C anneals. The point at which the density starts to increase is equal to the temperature at which the irradiation occurred (100–150°C and 500–550°C).

More than 30 fibers per condition were tensile tested per ASTM 3379-75 [25] on an Instron TM™ [4] with data collected using Labview™ software. Fiber axial displacements were measured with a Keyence™ [5] laser micrometer and loads were measured using a 1 kg Sensotec™ load cell. Density was measured using a density gradient column [26] and chemicals were mixed to generate several different columns. One column with a density range between 2.90 and 3.1 g/cm^3 was mixed for the Sylramic fiber with bromoform and diiodomethane. A second column measured densities between 2.70 and 2.9 g/cm^3 for the Hi-Nicalon fiber and was mixed with bromoform and ethyl bromide. A third column measured densities between 2.50 and 2.8 g/cm^3 for the cg Nicalon fiber and was mixed with bromoform and ethyl bromide.

Fiber transmission electron microscopy (TEM) specimens were made by gluing sectioned pieces of the fiber bundles together to make a compact plate which was progressively thinned, polished and ion milled. TEM was performed on a Philips CM-12 or CM-30. X-ray diffraction (XRD) specimens were made by crushing a fiber bundle to make a powder. Cu Kα radiation via a rotating anode was used; Cu Kα_2 and a continuously increasing background were removed from the XRD patterns using JADE™ software.

3. Analysis

3.1. Single fiber tensile testing

Single fiber testing determined a mean strength, Young's modulus and a Weibull modulus (m). Mean strength and Young's modulus were calculated from load (F), displacement (δ), gage length (L) and diameter (d) measurements. A typical load–displacement curve is shown in Fig. 2.

The failure stress, σ_f, is $F_{max}/(\pi d^2)$ where F_{max} is the load at failure. The mean failure stress is taken as the arithmetic mean for the irradiation condition. For all conditions tested, thirty or more specimens were tested, to reduce sampling errors [27]. Fibers that failed at the grip-fiber interface were discarded from the analysis. Each of the fiber diameters was measured in a Philips XL 30 scanning electron microscope (SEM) and all measurements were made at the same working distance. Weibull analysis was performed per ASTM C1239-95 [28].

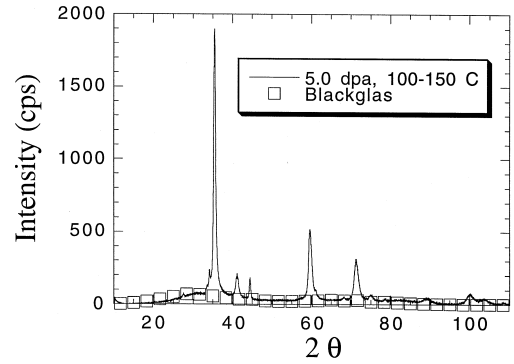

Fig. 3. Intensity versus 2θ for irradiated Sylramic and scattering due only to short range order from Blackglas.

[4] Trademark of Instron Corp., Canton, MA.
[5] Trademark of Keyence Corp., Fair Lawn, NJ.

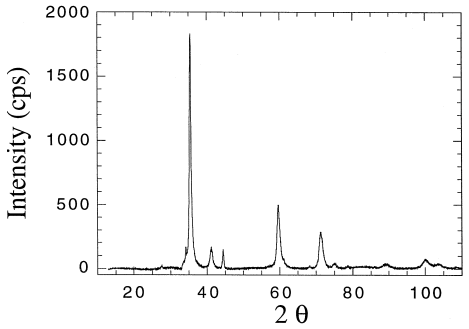

Fig. 4. Intensity versus 2θ for irradiated Sylramic with scattering due to short range order removed.

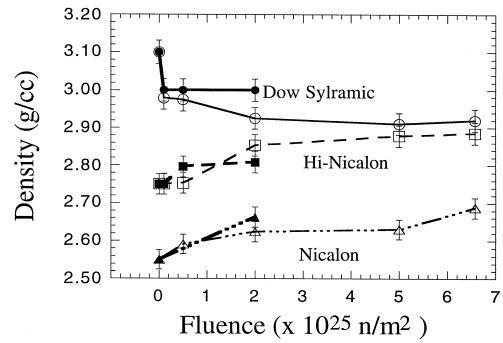

Fig. 5. Density changes with fluence.

The Weibull modulus is a number that gives a relative measure of the scatter in the data much like a standard deviation. However, whereas the standard deviation is an absolute number, the Weibull modulus is dimensionless. The three parameter Weibull distribution function is given by

$$P = 1 - \exp\left(-q\left(\frac{\sigma - \sigma_u}{\sigma_0}\right)^m\right), \tag{6}$$

where P is the cumulative probability of failure, q is the number of links for the fiber length, m is the shape parameter (Weibull modulus), σ_0 is a scaling parameter, σ is the applied stress and σ_u is the threshold stress (stress below which the fibers will not break). Eq. (6) is valid for a single type of flaw population and for time independent strength (no creep). To determine the probability of failure, P, at each stress, an estimator equation is used. The stresses are arranged in ascending order and the estimator is used to determine P for the ith stress. There are various estimators but the one which gives the least biased estimation of m is as [27]

$$P = \frac{(i - 0.5)}{N}, \tag{7}$$

where N is the total number of samples tested and i represents one of these samples. The Weibull modulus is calculated as the slope of a straight line in $\ln - \ln(1/(1 - P))$ versus $\ln \sigma$ space [29–32].

3.2. X-ray diffraction

From the XRD measurements, the degree of long range order was calculated by subtracting out a fit of an amorphous Si–C–O glass (Blackglas™ [6]) pattern from the partially crystalline pattern and then integrating the intensities over 2θ for each of the patterns. Blackglas was used because it is amorphous and has the same elements as the fibers' non-silicon carbide regions. This means that the X-ray absorption by the Blackglas and any of the SiC fibers is approximately equivalent. The progression is shown in Figs. 3 and 4. Peak fitting, separation of overlapping peaks and Warren–Averbach analysis were performed using software developed at the High Temperature Materials Laboratory (HTML) in Oak Ridge [33,34]. The reference peaks were measured from a small cylindrical chemical vapor deposition (CVD) SiC specimen which had grains of several microns in diameter and was oriented such that there were no sub-peaks due to stacking faults (pseudo-polymorphs).

4. Results

4.1. Physical and mechanical properties

Post-irradiation testing showed large changes in the fiber properties; density, elastic modulus, mean strength and Weibull modulus, which are presented in Figs. 5–8. From the density gradient column, fiber density data (Fig. 5) indicated that the cg Nicalon fiber and Hi-Nicalon fiber densified while the Sylramic fiber swelled. This is assuming negligible mass changes in the fibers. The Sylramic fiber swells three times as much as the CVD SiC for both

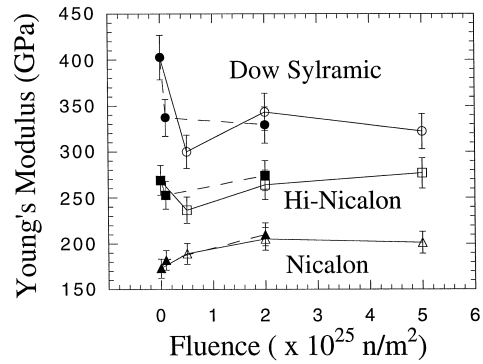

Fig. 6. Mean Young's modulus versus fluence.

[6] Trademark of Allied Signal Corp.

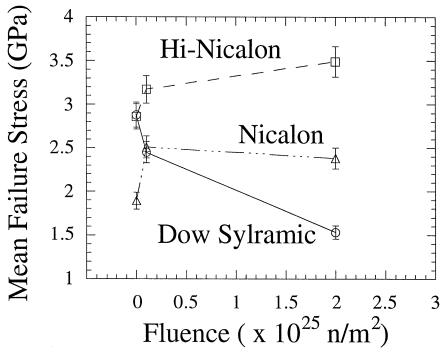

Fig. 7. Mean failure strength versus fluence (T_{irr} = 500–550°C).

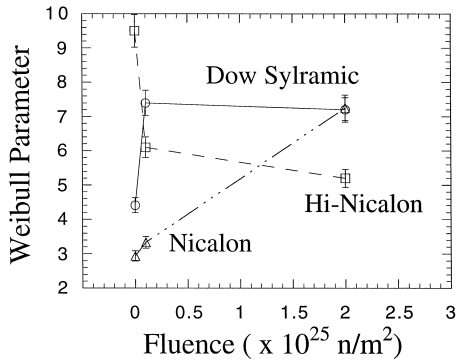

Fig. 8. Weibull modulus versus fluence (T_{irr} = 500–550°C, error bars represent 90% confidence interval).

temperature ranges [35]. The volume change of CVD SiC is calculated from the density changes of CVD SiC temperature monitors, Fig. 1. The initial density of the two monitors, 3.155 and 3.115 g/cm^3, coupled with unirradiated CVD SiC, 3.19 g/cm^3, translates to 1.2 and 2.4% volume change. These volume changes correspond to the Price data [18]. These volume change measurements are qualitatively supported by average fiber diameter measurements [36]. Single fiber tensile testing and SEM fiber diameter measurements allowed calculation of elastic modulus changes with fluence, Fig. 6. It was found that the Sylramic fiber again behaves similarly to CVD SiC [35] with both having about a 15 to 20% decrease in elastic modulus value. In contrast, the Hi-Nicalon fiber had little change in elastic modulus and the elastic modulus of the cg Nicalon fiber increased.

The density and elastic modulus changes for the fibers showed consistent trends for both irradiation temperatures, meaning that the property went up or down in the same manner for the fiber in question. Therefore, only the higher temperature irradiation data are presented in Figs. 7 and 8 because there are deviations from these trends in Sylramic fiber strength and Weibull modulus. The low temperature data are presented in Table 2.

The fluence dependence of mean failure strength at the higher irradiation temperature is presented in Fig. 7. For both the Hi-Nicalon fiber and the cg Nicalon fiber, the strength for both types of fibers increased with fluence above their unirradiated values with the cg Nicalon showing signs of plateauing while the Hi-Nicalon continually increases. This trend is similar to their low temperature irradiation behavior. The Sylramic fiber strength decreased by about half for a dose of about 2 dpa. This change in the Sylramic fiber strength is opposite to the trends shown in Figs. 5 and 6.

Examination of the Weibull moduli plotted in Fig. 8 shows that the Hi-Nicalon fiber and cg Nicalon fiber had relatively smooth transitions as dose increased. The Hi-

Table 2
Low temperature (T_{irr} = 100–150°C) bulk properties of SiC type fibers. Errors for Table 2 are as follows: the standard error for strength is ±3%, 95% confidence on the Young's modulus (calculated from the slope of the load–displacement curve) ±0.5% while experimental error would be closer to 8%, 90% confidence for the Weibull modulus is ±15% and for the density the experimental error is ±1%

Fiber type		Neutron fluence ($\times 10^{25}$ n/m^2)					
		0.0	0.1	0.5	2.0	5.0	6.6
Sylramic	mean strength (GPa)	2.88	2.38	2.64	2.83	2.83	
	mean modulus (GPa)	403	296	300	343	322	293
	Weibull modulus	4.21	3.65	4.06	3.86	3.63	
	density (g/cm^3)	3.1	2.98	2.97	2.93	2.91	2.92
Hi-Nicalon	mean strength (GPa)	2.86	2.89	3.20	3.19	3.63	3.91
	mean modulus (GPa)	267	231	237	264	277	272
	Weibull modulus	9.07	7.00	4.87	3.92	3.25	
	density (g/cm^3)	2.75	2.75	2.75	2.85	2.88	2.89
cg Nicalon	mean strength (GPa)	1.89		2.84	2.87	2.78	2.30
	mean modulus (GPa)	173		189	205	201	196
	Weibull modulus	2.81		3.60	3.77	4.98	
	density (g/cm^3)	2.55		2.59	2.62	2.63	2.69

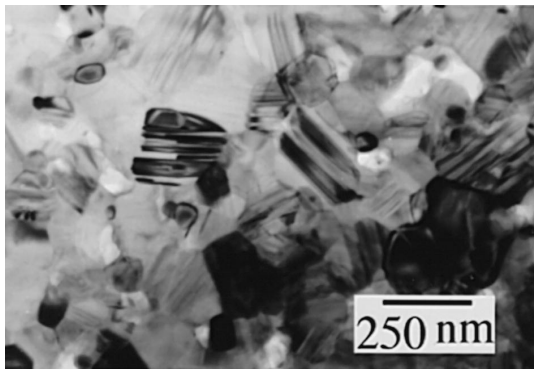

Fig. 9. TEM image of unirradiated Sylramic.

Nicalon fiber Weibull modulus decreased and the cg Nicalon fiber Weibull modulus increased, both by about a factor of two. The Sylramic fiber exhibited a step increase in the Weibull modulus at the lowest irradiation fluence in this study (0.1×10^{25} n/m^2), almost doubling from the unirradiated value (4 to 7.2).

Comparing Figs. 7 and 8 to the data given in Table 2, one can see that there are significant changes in the Sylramic fiber tensile properties from the low to the higher irradiation temperature. Specifically, at the low irradiation temperature, the Sylramic fiber strength and Weibull modulus did not effectively change. Conversely, the strength and Weibull modulus for the Sylramic fiber changed significantly after the 500–550°C irradiations with a 50% decrease in strength and the Weibull modulus nearly doubling when compared to the unirradiated values.

For the Hi-Nicalon fiber and cg Nicalon fiber, comparing Table 2 and Figs. 7 and 8, similar trends are observed. The strength increased and Weibull modulus decreased for the Hi-Nicalon fiber but the changes were not as much for the higher temperature irradiation as for the lower. For the cg Nicalon fiber, the strength did not increase as much at the higher irradiation temperature but the Weibull modulus increased more at the higher irradiation temperature than at the low irradiation temperature.

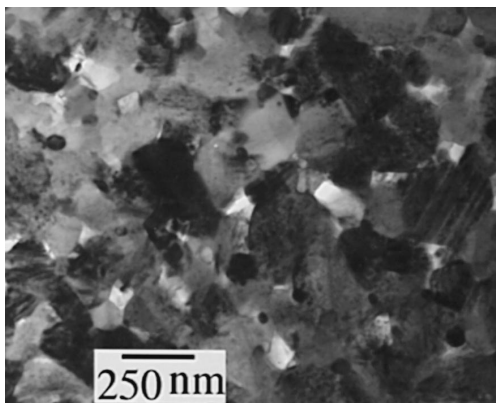

Fig. 10. TEM image of irradiated Sylramic.

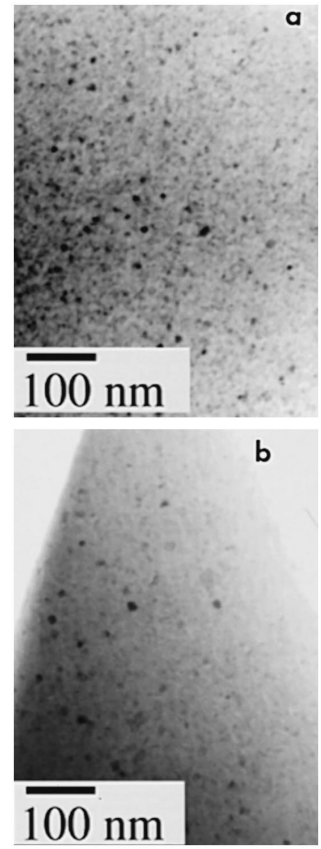

Fig. 11. TEM image of Hi-Nicalon: (a) unirradiated Hi-Nicalon; (b) irradiated Hi-Nicalon (5 dpa, 100–150°C).

4.2. Microstructure

Low magnification TEM images of the Sylramic fiber and Hi-Nicalon fiber are shown in Figs. 9–11 for an irradiated and an unirradiated condition. These images are representative of all the irradiation conditions investigated.

From the images one can see that both the Sylramic fiber and the Hi-Nicalon fiber grain size has apparently not changed. The Sylramic fiber has visible black spot damage

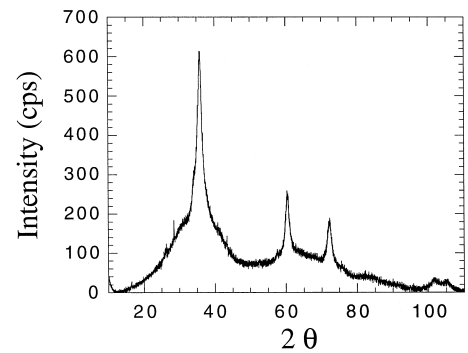

Fig. 12. XRD of Hi-Nicalon irradiated to 5 dpa, $T_{irr} = 100–150$°C.

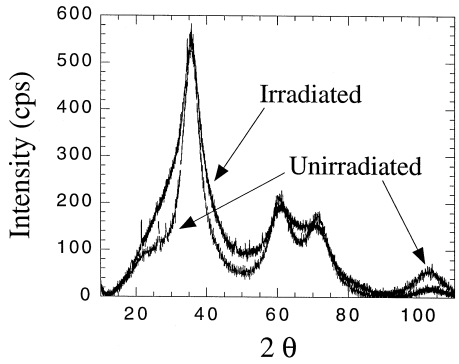

Fig. 13. XRD of unirradiated cg Nicalon and irradiated cg Nicalon (0.5 dpa, T_{irr} = 500–550°C).

while the Hi-Nicalon fiber seems to have less grains following irradiation but because of the very small grain size, only relative/qualitative changes can be established. Quantitative data can not be obtained from any of these images since due to the very small grain size there will be overlapping of grains through the imaged thickness and different diffraction conditions for each of these grains. Additional useful crystallographic information can be easily obtained and quantified via XRD. Fig. 3 shows typical XRD of Sylramic fibers due to neutron irradiation. There is a marked difference between the XRD patterns of Sylramic fiber and those of cg Nicalon fiber or Hi-Nicalon fiber as shown in Figs. 12 and 13. Specifically, the degree of long range ordering is much less for the Hi-Nicalon fiber and even less for the cg Nicalon fiber. cg Nicalon fiber irradiated to 2 dpa at 100–150°C is an extreme case because it appears completely amorphized. The data obtained for Sylramic fiber and Hi-Nicalon fiber from XRD are presented in Table 3.

5. Discussion

Radiation damage produces point defects and small defect clusters in SiC which causes swelling as seen by the increase in the lattice parameter. The lattice parameter changes also relate to the elastic modulus, since lattice expansion causes an increase in the interatomic distance. With the increase in the atomic separation, the curvature of the atomic bonding energy versus atomic separation decreases giving a lower stiffness. As can be seen in Table 3, the uniform strain for the Sylramic fiber irradiated at

Table 3
XRD results for Sylramic and Hi-Nicalon. The repeat length and rms microstrain are for the {111}

Property measured	Fluence ($\times 10^{25}$ n/m^2)	Sylramic T_{irr} = 500–550°C	Sylramic T_{irr} = 100–150°C	Hi-Nicalon T_{irr} = 100–150°C	Hi-Nicalon T_{irr} = 500–550°C
Percent long range SiC ordering	0.0	100	100	90	90
	0.1	84	85		80
	0.5		60	50	
	2.0	65			80
	5.0		60	30	
Repeat length via Warren–Averbach (Å)	0.0	1199	1199	50	50
	0.1	758	334	no effective change in FWHM	no effective change in FWHM
	0.5		252		
	2.0	162			
	5.0		128		
R.m.s. microstrain	0.0	0.0006	0.00060	0.0005	0.0005
	0.1	0.0009	0.00151	no effective change in FWHM	no effective change in FWHM
	0.5		0.00056		
	2.0	0.0023			
	5.0		0.00048		
Uniform strain ($\Delta a/a$)	0.0	0.0000	0.0000		no effective change in peak positions
	0.1	0.0072	0.0105		
	0.5		0.0138	(+)[a]	
	2.0	0.0060			
	5.0		0.0058	(−)[a]	

[a]Although there were peak position changes (specifically the higher 2θ peaks), the lattice parameter was not quantified due to considerable error from subtracting out the short range order effect.

100–150°C increases then decreases after 0.5 dpa which corresponds with the Young's modulus data decrease then increase of Fig. 6.

For the Hi-Nicalon fiber and cg Nicalon fiber, a different phenomenon is occurring. The grains are very small as shown in Fig. 11 so they can not collect any substantial number of point defects. This is known because the SiC peaks do not change position with 2θ and they do not change their breadth, Table 3. Both of these fiber types, however, lose a large degree of their long range crystalline order. The XRD results coupled with TEM observations indicate that there are less SiC crystallites in Hi-Nicalon fiber and that the fibers are becoming amorphous. With less SiC crystallites, the elastic modulus decreases (crystalline is stiffer than glass) which is seen initially in the Hi-Nicalon fiber. As damage increases, the fibers densify and this effect in the Hi-Nicalon fiber equals or slightly out-weighs the loss of crystallinity effect therefore the elastic modulus returns to its original level. This effect should also happen in the cg Nicalon fiber but the densification effect swamps out any loss of crystallinity so the elastic modulus will increase. In the Hi-Nicalon fiber, it is the excess carbon (Table 1) which is densifying since SiC is known to expand when irradiated, as mentioned in Section 4. The exact crystallographic configuration of the carbon atoms is as yet unknown. The cg Nicalon fiber has excess oxygen (Table 1) which crosslinks the polymer to prevent melting during pyrolysis. The Si–C–O non-crystalline mixture is the phase that would be expected to densify during irradiation [37]. Changes in the cg Nicalon fiber will be similar to the changes occurring in the Hi-Nicalon fiber; compaction of a non-crystalline phase with amorphization of nano-crystallites.

The strength changes in the Hi-Nicalon fiber and cg Nicalon fiber can be explained by radiation-induced densification. The load carrying capacity per unit length of the Hi-Nicalon fiber does not change until the highest damage level tested in this study but the measured diameter continually decreased with increasing damage, therefore the strength increased. For the cg Nicalon fiber, the strength also increases as a result of the fiber diameter becoming smaller. After 2 dpa at the lower irradiation temperature, the load carrying capacity per unit length of the cg Nicalon fiber decreases resulting in a strength maximum near 2 dpa.

For the Sylramic fiber, the strength does not change much after the low temperature irradiation. The strength initially decreases which is a volumetric effect due to the swelling of the SiC as measured by the fiber diameter. The fiber diameter increases to a maximum value due to point defect production and then starts to decrease from this value as the point defects agglomerate to form damage spots visible with TEM. These diameter changes correspond to the changes in the uniform strain (lattice parameter). Therefore, the fiber strength which is inversely proportional to fiber diameter squared increases again from a low around 0.5 dpa as the fiber diameter decreases. But, with no measurable change in the Weibull modulus, the flaw distribution controlling failure of these fibers apparently remains the same.

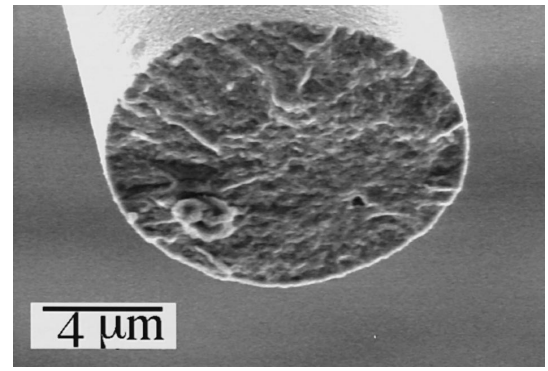

Fig. 14. SEM of unirradiated Sylramic fracture surface.

This is not the case after higher temperature irradiations. The Weibull parameter for the Sylramic fiber shows a step increase, 4.2 to 7.2, from the lowest damage level of 0.1 dpa. A gradual change in Weibull modulus signifies that there is a refinement in either direction of the strength-controlling flaw distribution. This effect is seen in the cg Nicalon fiber and Hi-Nicalon fiber data. For the Sylramic fiber, the change in fracture mechanisms is also apparent by the change in the fracture surfaces, shown in Figs. 14 and 15. Qualitative descriptions of the unirradiated surface indicate classical brittle fracture features, while the irradiated surface can be described as 'spongy' and 'pitted'. Neither of these fibers failed due to surface flaws so their microstructural characteristics are likely responsible for the different fracture behaviors.

The new controlling flaw distribution in the irradiated Sylramic fibers resulted in less scatter in the strength data along with a reduction in the strength. Therefore the flaws in the irradiated fibers must be larger than the previous flaws or in a different location. This now leads one to look

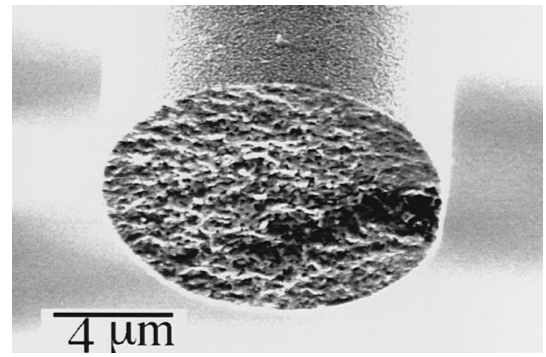

Fig. 15. SEM of irradiated Sylramic fracture surface (2.0 dpa, $T_{irr} = 500–550°C$).

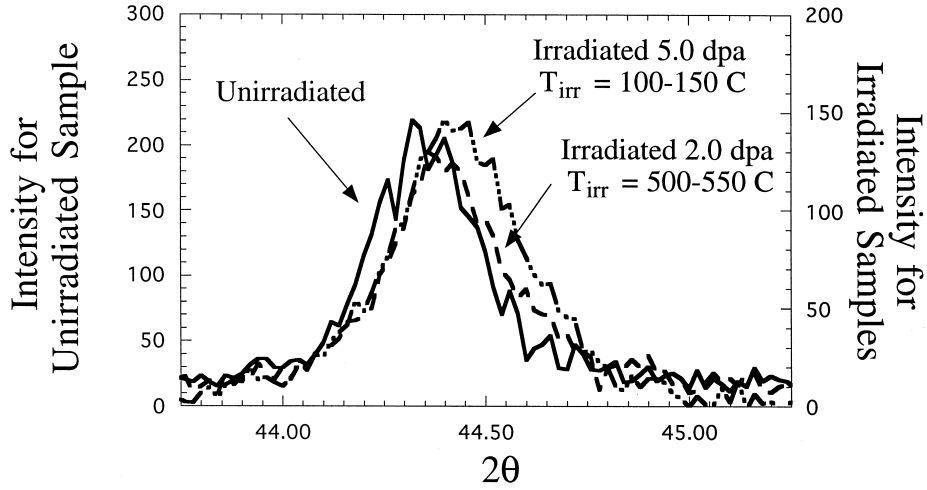

Fig. 16. XRD of TiB_2.

at the effect of neutrons on TiB_2. B^{10} is converted to Li^7 by reacting with thermal neutrons and all B^{10} is completely transmuted for all the irradiation conditions tested. The quantity of boron converted is about 20%, since 19.9% of naturally occurring B is B^{10}. The α particle (He nucleus) and Li produced from the transmutation are ejected from the TiB_2 inclusion. The recoil energy of the particles due to the mass difference of the reaction is large enough to cause the particles to penetrate into the SiC grains of the fiber. With the removal of such a large fraction of its constituency, the lattice of the TiB_2 would naturally contract which is shown in the XRD, Fig. 16, by a peak shift to higher 2θ and a slightly broader peak. This effect is observed at the low temperature irradiations. At the higher temperature irradiations, the peaks do not shift as much and they do not broaden.

A possible explanation for the strength decrease of Sylramic fiber and XRD changes after irradiation would be that the TiB_2 phase is starting to transform into a more stable form or phase. The Ti–B phase diagram reveals that there are other stable forms of Ti and B. For the concentration change in the TiB_2 particles (66 to 53.4 at.% B), the stable forms would be TiB and Ti_3B_4. Thermodynamically there is a large driving force but kinetically it is a sluggish reaction, inferred from the phase diagram [38]. At the low temperature irradiations, the transformation will not occur. At slightly higher temperatures, the TiB_2 could begin transformation. The TiB_2 should transform into about half TiB and half Ti_3B_4. Although there is some debate on the existence of Ti_3B_4 [38], the combination of these two phases has a larger volume per atom than TiB_2, 45 to 30 $Å^3$/atom (PDF cards, 19-1368, 05-0700, 35-0741). As the TiB_2 inclusion begins to transform to TiB and Ti_3B_4, the inclusion starts to expand but due to being restricted to a finite volume the transformation does not readily occur. However, tensile stresses are exerted on the SiC grain boundaries surrounding the TiB_2 particles. Therefore, a reduction in failure strength and increase in Weibull modulus would be expected. Since the particle can not readily reform at the low temperature, the XRD peak exhibits a greater peak shift and broadening (contracted lattice leads to peak shift to higher 2θ and smaller particles leads to broader peaks). At the higher irradiation temperature, the XRD peak location is slightly shifted for the irradiated case; the lattice has not contracted from the unirradiated condition. The XRD peak breadth for the irradiated condition is slightly less than the unirradiated condition suggesting slightly larger particles. Further study is needed to fully confirm the above conjectures.

In regard to the effect of fiber property changes on composite behavior, volumetric changes will have significant effects on the residual stresses in the fiber, matrix and interface. These effects are important but are discussed elsewhere in regard to the matrix property changes [35] as this study was primarily concerned with fiber property changes.

Dimensional changes in the fibers, particularly fiber shrinkage, will have the greater effect on the matrix cracking stress when not considering the residual stresses. The shrinkage for cg Nicalon is about 4 to 4.5 vol.% after irradiation to 2 dpa at 500–550°C as shown in Fig. 5. It has been shown that radiation damage of cg Nicalon fiber reduces the interfacial strength of a 30/60/90 SiC CFCC with a carbon interface [13,39]. This reduction in interfacial strength should severely reduce the matrix cracking stress given in Eq. (1) which would offset any advantages gained by increasing the fiber elastic modulus or decreasing fiber radius. The amount of pullout was reported to increase [13] with a decrease in the interfacial strength which follows from Eqs. (4) and (5).

Now considering the Hi-Nicalon fiber, the volumetric shrinkage is about 2.2% for the same temperature range.

Therefore one would expect that the interfacial strength decrease would be less than for the cg Nicalon fiber assuming that the interface was not affected by the neutrons. There should be a corresponding increase in the amount of pullout for this case over the unirradiated case. With all CFCCs, the interfacial strength changes need to be measured to make better assessments of composite property changes.

Lastly considering the Sylramic fiber, the fiber swells about 3.5% at the same irradiation temperature which is similar in behavior to monolithic SiC swelling. The result is that the interface should not weaken as it would for the cg Nicalon fiber and Hi-Nicalon fiber. The matrix cracking stress variations would not be dominated by the interfacial changes but would vary due to small effects in all of the parameters as given by Eq. (1).

In regard to the composite, ultimate uniaxial tensile strength made with Sylramic fiber, this property should decrease after irradiation at a slightly elevated temperature (500°C) by about 50%. Making the assumption that the uniaxial composite has 40 vol.% fibers, the ultimate tensile strength should be approximately 400–500 MPa. This would still make a composite usable since it would not crack and fail simultaneously with matrix cracking stresses generally between 100–200 MPa [40]. A major question is how these fibers perform at even higher damages (>20 dpa) or at even higher irradiation temperatures (near 1000°C).

Considering the ultimate tensile strength of uniaxial composites using cg Nicalon or Hi-Nicalon, these values for both types of fibers should increase. If the matrix cracking stress for composites with these fibers decreases after irradiation below a design level, 140 MPa for ARIES [41], they will not be usable due to loss of hermeticity.

6. Conclusions

After irradiation of cg Nicalon, Hi-Nicalon and Sylramic fibers at irradiation temperatures of 100–150°C and 500–550°C with fluences for both temperature ranges $\leq 5 \times 10^{25}$ n/m^2, the following conclusions have been reached.

(1) cg Nicalon fiber has significant fiber shrinkage which can lead to the fiber pulling away from the interface in a composite which will result in a very low matrix cracking stress and increased fiber pullout. Overall, the mechanical properties, strength and elastic modulus, have lower values than for more stoichiometric SiC fibers. cg Nicalon fibers irradiated below 5 dpa and below 500–550°C have tensile strengths of 2–2.5 GPa, Young's moduli of 150–200 GPa and densities of 2.5–2.65 g/cm^3.

(2) Hi-Nicalon fiber has adequate mechanical properties, higher strength (3–3.5 GPa) and elastic modulus (240–280 GPa) than cg Nicalon fiber and its properties are relatively stable in a radiation field. However, the shrinkage (2.2 vol.%) of the fiber is still considered to be detrimental for composite performance due to assumed interfacial weakening.

(3) Density and elastic modulus changes of Sylramic fiber are similar to irradiated bulk SiC. The density decreased about 6% and the elastic modulus decreased about 20%. Sylramic fiber also exhibits significant mean strength reduction between high and low temperature irradiations; 3 to 1.5 GPa. This degradation can be rationalized by an assumed radiation assisted transformation of the TiB_2 particles present in the material. Further study is required. Even with the strength reduction, the fiber could potentially still be used for composites in a neutron field at low irradiation temperatures and low damage levels since the ultimate tensile strength of the composite should still be well above the critical matrix cracking stress.

References

[1] G.P. Pells, J. Nucl. Mater. 122&123 (1984) 1338.
[2] F. Porz, G. Grathwohl, F. Thummler, Mater. Sci. Eng. 71 (1985) 273.
[3] M. Okada, T. Noda, F. Abe, J. Nucl. Mater. 169 (1989) 249.
[4] L.H. Rovner, G.R. Hopkins, Nucl. Technol. 29 (1976) 274.
[5] L.L. Snead, R.H. Jones, A. Kohyama, P. Fenici, J. Nucl. Mater. 233–237 (1996) 26.
[6] J. Linke, H. Hoven, K. Koizlik, H. Nickel, E. Wallura, High Temp. High Press. 21 (1989) 533.
[7] R.H. Jones, C.H. Henager, J. Nucl. Mater. 219 (1995) 55.
[8] R.H. Jones, C.H. Henager, J. Nucl. Mater. 212–215 (1994) 830.
[9] G.W. Hollenburg, R.H. Jones, G.E. Lucas, Fusion Technol. 19 (1991) 1701.
[10] G.R. Hopkins, J. Chin, J. Nucl. Mater. 141–143 (1986) 148.
[11] H. Kodama, T. Miyoshi, J. Am. Ceram. Soc. 73 (1990) 3081.
[12] K. Niihara, Am. Ceram. Soc. Bull. 63 (1984) 1160.
[13] G.W. Hollenburg et al., J. Nucl. Mater. 219 (1995) 70.
[14] M.C. Osborne, L.L. Snead, D. Steiner, J. Nucl. Mater. 219 (1995) 63.
[15] B. Budiansky, J.W. Hutchinson, A.G. Evans, J. Mech. Phys. Solids 34 (1986) 167.
[16] W.A. Curtin, Composites 24 (1993) 98.
[17] R. Blackstone, E.H. Voice, J. Nucl. Mater. 39 (1971) 319.
[18] R.J. Price, J. Nucl. Mater. 33 (1969) 17.
[19] R.J. Price, J. Nucl. Mater. 48 (1973) 47.
[20] W. Primak, L.H. Fuchs, P.P. Day, Phys. Rev. 103 (1956) 1184.
[21] R.W. Davidge, in: K. Friedrich (Ed.), Applications of Fracture Mechanics to Composite Materials, Elsevier, New York, 1989, p. 547.
[22] J. Lipowitz, J.A. Rabe, A. Zangvil, Y. Xu, Ceram. Eng. Sci. Proc. 18 (1997) 147.
[23] M. Takeda, J. Sakamoto, A. Saeki, Y. Imai, H. Ichikawa, Ceram. Eng. Sci. Proc. 16 (1995) 37.
[24] R.J. Price, Nucl. Technol. 16 (1972) 536.
[25] D3379-75 Tensile Strength and Young's Modulus for High Modulus Single Filament Materials, in: Annual Book of ASTM Standards, ASTM, West Conshohocken, PA, 1996, p. 125.

[26] D1505-85 Density of Plastics by the Density-Gradient Technique, in: Annual Book of ASTM Standards, ASTM, West Conshohocken, PA, 1985.
[27] W. Bergman, J. Mater. Sci. Lett. 3 (1984) 689.
[28] C1239-95 Standard Practice for Reporting Uniaxial Strength Data and Estimating Weibull Distribution Parameters for Advanced Ceramics, in: Annual Book of ASTM Standards, ASTM, West Conshohocken, PA, 1995.
[29] W. Weibull, J. Appl. Mech. (1951) 293.
[30] S.N. Patankar, J. Mater. Sci. Lett. 10 (1991) 1176.
[31] E.M. Asloun, J.B. Donnet, G. Guilan, M. Nardin, J. Schultz, J. Mater. Sci. 24 (1989) 3504.
[32] A.K. Di, K.K. Phani, J. Composite Mater. 24 (1990) 220.
[33] C.R. Hubbard, B. Morosin, J.M. Stewart, XRAYL: A program for producing idealized powder diffraction line profiles from overlapping powder diffraction lines, Oak Ridge National Laboratory, Oak Ridge, TN, 1996.
[34] C.R. Hubbard, B. Morosin, J.M. Stewart, CRYSIZ: A program for computing crystallite size and strain from the broadening of powder diffraction lines, Oak Ridge National Laboratory, Oak Ridge, TN, 1996.
[35] M.C. Osborne, J.C. Hay, L.L. Snead, J. Am. Ceram. Soc. (1997) to be submitted.
[36] M.C. Osborne, Neutron irradiation effects on the microstructure and mechanical and physical properties of monolithic silicon carbide and silicon carbide fibers, thesis, Rensselaer Polytechnic Institute, 1997, to be submitted.
[37] L.L. Snead, M.C. Osborne, K.L. More, J. Mater. Res. 10 (1995) 736.
[38] J.L. Murray, P.K. Liao, K.E. Spear, in: T.B. Massalski (Ed.), Binary Alloy Phase Diagrams, ASM International, Materials Park, OH, 1990, p. 544.
[39] L.L. Snead, S.J. Zinkle, D. Steiner, J. Nucl. Mater. 191–194 (1992) 566.
[40] A.G. Evans, F.W. Zok, J. Mater. Sci. 29 (1994) 3857.
[41] The Aries-I Tokamak Reactor Study, UCLA-PPG-1323, 1991.